ChemComm

COMMUNICATION

View Article Online
View Journal | View Issue

Cite this: *Chem. Commun.*, 2019, 55, 13820

Received 10th September 2019,
Accepted 21st October 2019

DOI: 10.1039/c9cc07085k

rsc.li/chemcomm

Cucurbit[8]uril-based supramolecular nanocapsules with a multienzyme-cascade antioxidative effect†

Shengda Liu,‡ Ruizhen Tian,‡ Jiayun Xu, Liang Wang, Jianxin Sun, Xiaojia Jiang, Tingting Wang, Xiumei Li, Quan Luo and Junqiu Liu *

A supramolecular nanocapsule was constructed by the ternary host–guest complexation of azobenzene (Azo) and methylviologen (MV) to cucurbit[8]uril (CB[8]) and the subsequent self-assembly. The supramolecular nanocapsule with both glutathione peroxidase (GPx) and superoxide dismutase (SOD) activities can mimic the intracellular enzymatic reactive oxygen species (ROS) defense system.

Reactive oxygen species (ROS), such as $O_2^{-\bullet}$, $^{\bullet}OH$, and H_2O_2, are by-products of aerobic metabolism.[1,2] A moderate amount of ROS plays an essential role in signal transduction and cellular redox homoeostasis.[3,4] However, the excessive levels of ROS in the body will damage the cellular structure and lead to numerous human diseases, such as neurodegenerative diseases, atherosclerosis and cancer.[5,6] In organisms, antioxidative enzymes such as superoxide dismutase (SOD) and glutathione peroxidase (GPx) have evolved as cellular antioxidative defenses against the oxidative stress of ROS.[7,8] To date, much effort has been dedicated to the development of artificial antioxidative enzymes for mimicking their function. For example, various artificial antioxidative enzymes such as carbon based derivatives, cerium based derivatives, melanin based derivatives and manganese porphyrin based derivatives have been designed with significant SOD activity.[9–14] Additionally, a large number of GPx mimics were reported with multi-GPx-like centers in the form of monomers or their supramolecular assemblies.[15–19] Nevertheless, the construction of a cooperative ROS defense system with both SOD and GPx functions to ensure the balance and health in biological organisms is still a challenge. It is well-known that SOD can catalyze the decomposition of $O_2^{-\bullet}$ to produce H_2O_2 and O_2, and GPx further reduces H_2O_2 to generate harmless products. The recent effort to build such a dual-enzyme cascade system based on 65-mer peptides remains a time-consuming work that needs to integrate complex protein engineering and chemical mutation methods.[20] Therefore, it is highly desired to develop a simple and effective method to construct an artificial enzyme with both SOD and GPx activity for the simulation of the intracellular enzymatic ROS defense system.

Recently, the rapid development of nanoscale science and supramolecular chemistry has promoted the in-depth study of nanoscale artificial enzymatic systems.[21–25] Cucurbit[*n*]uril-based supramolecular assembly appears to be a promising method to prepare functional biological materials, such as a multienzyme-cooperative antioxidative system.[26–29] As a member of the cucurbit[*n*]uril (CB[*n*]) family, cucurbit[8]uril (CB[8]) is known to form a ternary host–guest complex with azobenzene (Azo) and methylviologen (MV), which seems to be an ideal platform to conjugate multiple enzymes of cascades in close proximity.[30–33] This model system has its own merits, including (1) CB[8] can combine two different molecules to introduce the catalytic centers of SOD and GPx. (2) The structural homogeneity of CB[8]-based supramolecular assembly can minimize the coupling deviation between enzyme parameters and structures. (3) The supramolecular assembly has good stability in the cell environment, which facilitates the study of antioxidants at the cell level.

Herein, a multienzyme-cascade model was constructed to simulate an intracellular enzymatic antioxidative defense system (Fig. 1). In this system, MV-modified manganese porphyrin derivative, 1,1′,1″,1‴-((manganese-porphyrin-5,10,15,20-tetrayltetrakis(pyridine-1-ium-4,1-diyl))tetrakis(pentane-5,1-diyl))tetrakis(1-methyl-[4,4′-bipyridine]-1,1′diium)octabromide tetraiodide (Mn-TMPP), acts as a SOD mimic while an Azo derivative containing selenoenzyme center, *N*,*N*′-(selenobis(ethane-2,1-diyl))bis(4-((*E*)-phenyldiazenyl)benzamide) (Se-bisAzo), serves as a GPx mimic. Since CB[8] can bind to Azo and MV from the two enzyme mimics, CB[8] is capable of forming heteroternary complexes with Mn-TMPP and Se-bisAzo for self-assembly into stable supramolecular nanocapsules. The formation mechanism of nanocapsules is consistent with the methodology reported in previous literature.[34–36] The obtained supramolecular nanocapsules hold SOD and GPx mimics together to achieve a synergistic antioxidative process, in which

State Key Laboratory of Supramolecular Structure and Materials, College of Chemistry, Jilin University, Changchun 130012, China. E-mail: junqiuliu@jlu.edu.cn

† Electronic supplementary information (ESI) available. See DOI: 10.1039/c9cc07085k

‡ These authors contributed equally to this work.

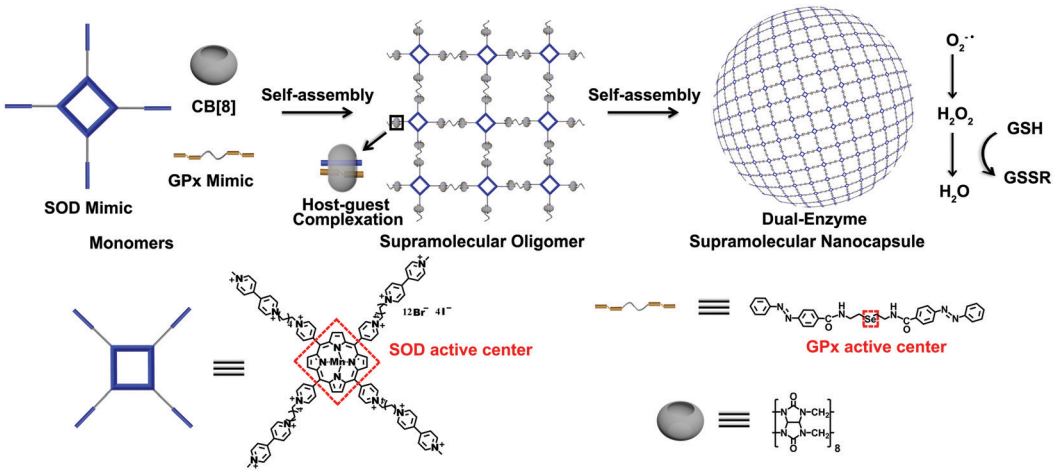

Fig. 1 Schematic illustration of the construction of the supramolecular nanocapsules with SOD and GPx activity.

the Mn-TMPP component catalyzes $O_2^{-\bullet}$ to produce H_2O_2 that is further decomposed by the Se-bisAzo component. The following *in vitro* experiments have confirmed that our nanocapsules have an admirable ability to remove intracellular ROS for cell protection under oxidative stress. This artificial enzyme model is able to simulate multienzyme-cooperative antioxidative defense systems in nature to protect the body from oxidative damage.

In order to prepare nanocapsules, Mn-TMPP, Se-bisAzo and CB[8] were mixed at a ratio of 1 : 2 : 4. The structure, morphology, and size of the nanocapsules were demonstrated by transmission electron microscopy (TEM), tapping-mode atomic force microscopy (AFM) and dynamic light scattering (DLS) analysis. From DLS data, nanocapsules showed an average diameter of 70 ± 30 nm (Fig. S12, ESI†). The size of these uniform spheres was also validated by TEM (Fig. 2A) and their shells can be observed directly when the samples were treated with phosphotungstic acid (Fig. 2B). In the high-resolution TEM image, the spheres exhibited a hollow interior structure with the shell thickness up to 3 nm (Fig. 2C). The AFM image further demonstrated the supramolecular spherical structure, the regular height of which was about 17 nm (Fig. 2D–F). These results clearly verified the hollow nanocapsules formed by supramolecular assembly.

As a dual-enzyme cascade system, the SOD and GPx activities of supramolecular nanocapsules were investigated. The SOD activity was firstly quantified by the xanthine oxidase/nitro blue tetrazolium (XOD/NBT) reduction assay established by Fridovich.[37] The enzymatic concentration that inhibits the production rate of methyl hydrazone by 50% (IC_{50}) is the concentration of one SOD active unit. The result showed that the IC_{50} value of supramolecular nanocapsules was measured to be 0.347 ± 0.014 μM (Fig. 3A), which is 0.375 ± 0.015% of the natural Cu–Zn-SOD.[38] Compared to the previously reported SOD mimic, such as manganese(III) *para*-tetrakis(*N*-methyl-pyridyl)porphyrin (Mn-TP) (IC_{50}: 0.670 μM), our supramolecular nanocapsules exhibited a relatively higher activity.[9] As for the GPx activity, the modified method developed by Hilvert was used to reduce cumene hydroperoxide (CUOOH) by utilizing

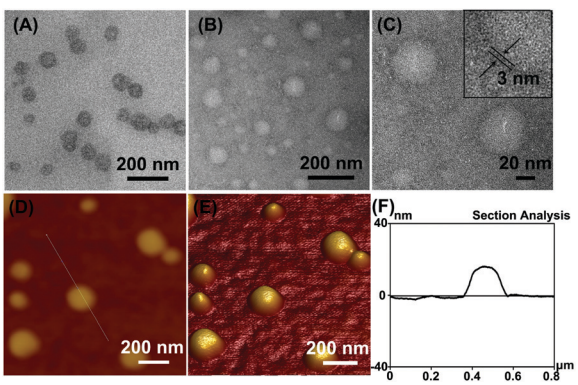

Fig. 2 Image of nanocapsules: (A and B) TEM image, (C) high-resolution TEM image, (D) AFM image, (E) 3D AFM image and (F) associated height curve along the black line in panel D. The samples of B and C were negatively stained with phosphotungstic acid.

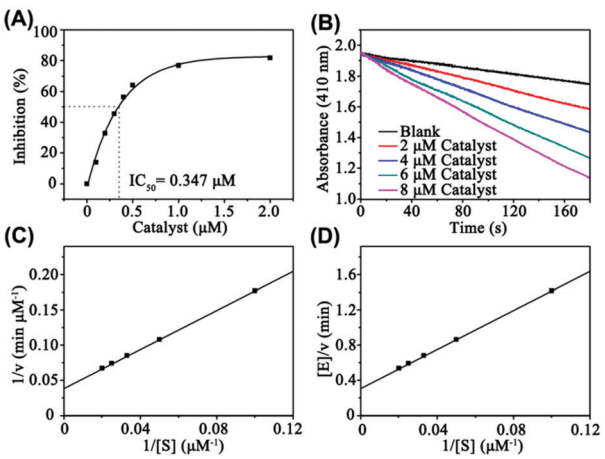

Fig. 3 GPx and SOD activities of supramolecular nanocapsules. (A) Percentage of inhibition of NBT oxidation by a superoxide anion radical *versus* different concentrations of supramolecular nanocapsules. (B) Plots of absorbance *versus* time during the catalytic reduction of CUOOH by TNB. (C and D) Lineweaver–Burk plots obtained for the catalyst of supramolecular nanocapsules.

Table 1 SOD and GPx activities of nanocapsules and other mimics

Samples	GPx activity[d]		SOD activity	
	V_0 ($\mu M\ min^{-1}$)	Relative activity	IC_{50} (μM)	Relative activity[f] (%)
Nanocapsules[a]	14.951	78 500	0.347	0.375
PhSeSePh[b]	0.011	1	n.d.	n.d.
Mn-TP[c]	n.d.[e]	n.d.	0.670	0.194

[a] The measurements of GPx or SOD activities are shown in the experimental method. [b] Activity values are based on ref. 40. [c] Activity values are based on ref. 9. [d] The concentration of GPx catalyst: nanocapsules (8 μM), PhSeSePh (462 μM) in the assay systems. [e] n.d. refers to no detection. [f] Percentage is calculated as a relative activity of SOD mimics against the native SOD. The native Cu–Zn SOD activity value is based on ref. 38.

3-carboxyl-4-nitrobenzenethiol (TNB) as a GSH substitute.[39] The catalytic rate can be calculated by monitoring the disappearance of TNB at 410 nm. As shown in Fig. 3B, supramolecular nanocapsules exhibited a GPx activity of 14.951 ± 0.748 μM min^{-1} (catalyst 8 μM). In contrast to the catalytic rate of other GPx mimics (PhSeSePh: 0.011 μM min^{-1}, catalyst 462 μM),[40] this supramolecular nanocapsule exhibited better ability to remove hydroperoxide (Table 1). The enzyme kinetics were further explored by determining the first-order rate constant (k_{cat}) and the apparent Michaelis constant (K_m) based on the following Michaelis–Menten equation:[41]

$$\frac{E_0}{\nu} = \frac{K_m}{k_{cat}} \cdot \frac{1}{[S]} + \frac{1}{k_{cat}}$$

$[E_0]$ is the enzyme concentration and [S] is the substrate concentration. K_m and k_{cat} were evaluated to be 34.70 ± 1.04 μM and 3.16 ± 0.18 min^{-1} at the TNB concentration of 150 μM, respectively. The corresponding second-order kinetic constant (k_{cat}/K_m) is (9.11 ± 0.81) × 10^4 M^{-1} min^{-1} (Fig. 3C and D). All the above results indicated that dual-enzyme cascade nanocapsules have been constructed successfully.

To apply the multienzyme-cascade antioxidative systems in real cellular environments, the cell uptake experiment of supramolecular nanocapsules was monitored by confocal laser scanning microscopy (CLSM). From Fig. 4A, supramolecular nanocapsules with red fluorescence (from Mn-TMPP) were observed in the cytoplasm, indicating that the nanocapsules can penetrate the mouse embryonic fibroblast (3T3 cell) membranes *via* endocytosis (Fig. 4A). The cytotoxicity of the supramolecular nanocapsules was then investigated by 3-(4,5-dimethylthiazol-2-yl)-2,5-diphenyltetrazolium bromide (MTT) assay at different concentrations with 3T3 cells for 24 hours incubation. As depicted in Fig. 4C, there were no significant changes in the relative survival rate when 3T3 cells were co-incubated with the supramolecular nanocapsules. The results indicated that this system shows almost no detectable cytotoxicity and can be applied as a biological material. In order to determine the intracellular ROS scavenging ability of the supramolecular nanocapsules, 3T3 cells were firstly pretreated with the nanocapsules and subsequently treated with Rosup. DCFH-DA was used as a fluorescent probe to detect the intracellular ROS level. In the control experiment, a high emissive fluorescence was observed when the cells were co-incubated

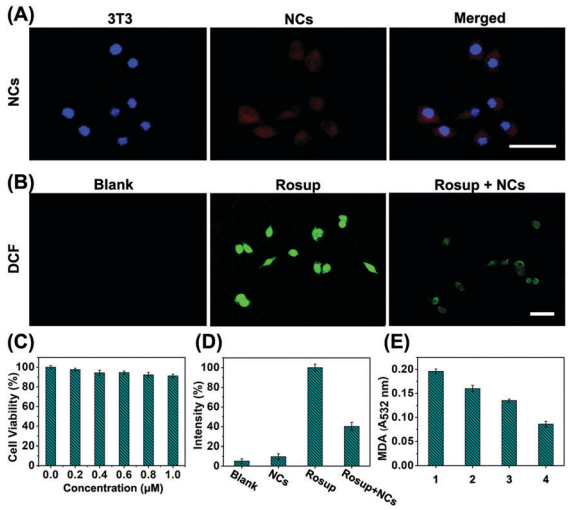

Fig. 4 (A) CLSM images of 3T3 cells after incubation with nanocapsules, cell nuclei stained with Hoechst (blue channel). The scale bar is 50 μm. (B) CLSM images of 3T3 cells with different treatments (Rosup or Rosup and nanocapsules). The scale bar is 50 μm. (C) MTT essay of relative cell viability of the 3T3 cells incubated with different concentrations of nanocapsules. (D) Effect of the nanocapsules on ROS scavenging in 3T3 cells. (E) Inhibition of MDA content treated with nanocapsules of different concentrations: (1) control (no nanocapsules), (2) 0.25 μM nanocapsules, (3) 0.5 μM nanocapsules, and (4) 1 μM nanocapsules.

with Rosup. In contrast, the fluorescence intensity was reduced when the Rosup-incubated cells were treated with the supramolecular nanocapsules. As shown in Fig. 4B, CLSM images demonstrated the antioxidative capability of the supramolecular nanocapsules. Furthermore, fluorescence analysis also indicated that the ROS can be removed by 59.9% when the sample was treated with the nanocapsules (1 μM) (Fig. 4D). The antioxidative ability of the supramolecular nanocapsules was further evaluated by a mitochondrial oxidative stress experiment. Malondialdehyde (MDA) is the characteristic product of lipid peroxides, which can be used to characterize the degree of lipid peroxidation. Therefore, the lipid peroxidation level of mitochondria was evaluated by detecting MDA production using a thiobarbituric acid (TBA) assay, which was monitored by the absorbance of the MDA–TBA adduct at 532 nm.[42] In this experiment, MDA was produced when the mitochondria were incubated with xanthine/XOD for 60 min. When multienzyme-cascade antioxidative supramolecular nanocapsules were added to the system and reacted for 60 minutes, the MDA content was partly inhibited. When the concentration of the added nanocapsules was 1 μM, the absorption reduced from 0.196 to 0.086 with an inhibition ratio of 56.1% (Fig. 4E). The above results indicated that the supramolecular nanocapsules with dual-enzyme activity can effectively remove ROS to protect organisms from oxidative damage.

In summary, we developed a strategy to construct supramolecular nanocapsules by self-assembly of the host–guest complexes of CB[8], Azo and MV. The supramolecular nanocapsules with both SOD and GPx activities can act as a multienzyme model to simulate an intracellular antioxidative defense system. The multienzyme-functionalized nanocapsules exhibited a significant

biological effect in removing intracellular ROS and protecting mitochondria against oxidative stress. We expected that this work could provide better understanding of the mechanism of the enzymatic antioxidative defense systems in organisms and promote the development of novel synergistic artificial enzymes for future applications in biology, medicine and materials.

This work was supported by the National Natural Science Foundation of China (No. 21420102007, 21574056, and 91527302).

Conflicts of interest

There are no conflicts to declare.

References

1 T. Wirth, *Angew. Chem., Int. Ed.*, 2015, **54**, 10074–10076.
2 C. C. Winterbourn, *Nat. Chem. Biol.*, 2008, **4**, 278–286.
3 M. Schieber and N. S. Chandel, *Curr. Biol.*, 2014, **24**, R453–R462.
4 T. S. Gechev, F. V. Breusegem, J. M. Stone, I. Denev and C. Laloi, *BioEssays*, 2006, **28**, 1091–1101.
5 H. Sies, *Angew. Chem., Int. Ed. Engl.*, 1986, **25**, 1058–1071.
6 H. Sies, *Exp. Physiol.*, 1997, **82**, 291–295.
7 L. A. Sena and N. S. Chandel, *Mol. Cell*, 2012, **48**, 158–167.
8 S. Hussain, W. Slikker Jr. and S. F. Ali, *Int. J. Dev. Neurosci.*, 1995, **13**, 811–817.
9 I. Batinic-Haberle, L. Benov, I. Spasojevic and I. Fridovich, *J. Biol. Chem.*, 1998, **273**, 24521–24528.
10 L. Yuan, S. Liu, W. Tu, Z. Zhang, J. Bao and Z. Dai, *Anal. Chem.*, 2014, **86**, 4783–4790.
11 K. Kamada and N. Soh, *J. Phys. Chem. B*, 2015, **119**, 5309–5314.
12 D. Jiang, D. Ni, Z. T. Rosenkrans, P. Huang, X. Yan and W. Cai, *Chem. Soc. Rev.*, 2019, **48**, 3683–3704.
13 J. Wu, X. Wang, Q. Wang, Z. Lou, S. Li, Y. Zhu, L. Qin and H. Wei, *Chem. Soc. Rev.*, 2019, **48**, 1004–1076.
14 F. Fucassi, J. E. Lowe, K. D. Pavey, S. Shah, R. G. Faragher, M. H. Green, F. Paul, D. O'Hare and P. J. Cragg, *J. Inorg. Biochem.*, 2007, **101**, 225–232.
15 X. Huang, X. Liu, Q. Luo, J. Liu and J. Shen, *Chem. Soc. Rev.*, 2011, **40**, 1171–1184.
16 Z. Dong, Q. Luo and J. Liu, *Chem. Soc. Rev.*, 2012, **41**, 7890–7908.
17 S. Shimodaira, T. Takei, H. Hojo and M. Iwaoka, *Chem. Commun.*, 2018, **54**, 11737–11740.
18 J. Li, C. Si, H. Sun, J. Zhu, T. Pan, S. Liu, Z. Dong, J. Xu, Q. Luo and J. Liu, *Chem. Commun.*, 2015, **51**, 9987–9990.
19 Y. Huang, C. Liu, F. Pu, Z. Liu, J. Ren and X. Qu, *Chem. Commun.*, 2017, **53**, 3082–3085.
20 J. Yin, J. Zhuang, S. Lv and Y. Mu, *J. Mol. Recognit.*, 2018, **31**, e2714.
21 N. Ma, F. Li, S. Li, S. Chu, L. Han, S. Liu, T. Yan, R. Tian, Q. Luo and J. Liu, *Nanoscale*, 2019, **11**, 3521–3526.
22 H. Zou, H. Sun, L. Wang, L. Zhao, J. Li, Z. Dong, Q. Luo, J. Xu and J. Liu, *Soft Matter*, 2016, **12**, 1192–1199.
23 J. Li, Z. Wang, J. Zhou, M. Li, Q. Luo, Z. Dong, S. Shi and J. Liu, *Colloids Surf., A*, 2018, **558**, 95–102.
24 Y. Yin, S. Jiao, C. Lang and J. Liu, *Soft Matter*, 2014, **10**, 3374–3385.
25 Y. Yin, S. Jiao, C. Lang and J. Liu, *RSC Adv.*, 2014, **4**, 25040–25050.
26 N. K. Shee, M. K. Kim and H. J. Kim, *Chem. Commun.*, 2019, **55**, 10575–10578.
27 C. Zhang, Y. Zhang, Z. Zhang, X. Wu, Q. Yua and Y. Liu, *Chem. Commun.*, 2019, **55**, 8138–8141.
28 X. Wu, Y. Chen, Q. Yu, F. Q. Li and Y. Liu, *Chem. Commun.*, 2019, **55**, 4343–4346.
29 K. M. Park, M. Y. Hur, S. K. Ghosh, D. R. Boraste, S. Kim and K. Kim, *Chem. Commun.*, 2019, **55**, 10654–10664.
30 C. Gao, Q. Huang, Q. Lan, Y. Feng, F. Tang, M. P. M. Hoi, J. Zhang, S. M. Y. Lee and R. Wang, *Nat. Commun.*, 2018, **9**, 2967.
31 C. Hu, N. Ma, F. Li, Y. Fang, Y. Liu, L. Zhao, S. Qiao, X. Li, X. Jiang, T. Li, F. Shen, Y. Huang, Q. Luo and J. Liu, *ACS Appl. Mater. Interfaces*, 2018, **10**, 4603–4613.
32 E. Pazos, P. Novo, C. Peinador, A. E. Kaifer and M. D. Garcia, *Angew. Chem., Int. Ed.*, 2019, **58**, 403–416.
33 F. Tian, D. Jiao, F. Biedermann and O. Scherman, *Nat. Commun.*, 2012, **3**, 1207.
34 D. Kim, E. Kim, J. Kim, K. M. Park, K. Baek, M. Jung, Y. H. Ko, W. Sung, H. Kim, J. H. Suh, C. G. Park, O. S. Na, D. K. Lee, K. E. Lee, S. S. Han and K. Kim, *Angew. Chem., Int. Ed.*, 2007, **46**, 3471–3474.
35 K. Baek, I. Hwang, I. Roy, D. Shetty and K. Kim, *Acc. Chem. Res.*, 2015, **488**, 2221–2229.
36 C. Sun, H. Zhang, L. Yue, S. Li, Q. Cheng and R. Wang, *ACS Appl. Mater. Interfaces*, 2019, **11**, 22925–22931.
37 J. M. McCord and I. Fridovich, *J. Biol. Chem.*, 1969, **244**, 6049–6055.
38 Y. Gao, C. Hou, L. Zhou, D. Zhang, C. Zhang, L. Miao, L. Wang, Z. Dong, Q. Luo and J. Liu, *Macromol. Biosci.*, 2013, **13**, 808–816.
39 Z. P. Wu and D. Hilvert, *J. Am. Chem. Soc.*, 1990, **112**, 5647–5648.
40 X. Huang, Y. Yin, Y. Tang, X. Bai, Z. Zhang, J. Xu, J. Liu and J. Shen, *Soft Matter*, 2009, **5**, 1905–1911.
41 H. Sun, L. Miao, J. Li, S. Fu, G. An, C. Si, Z. Dong, Q. Luo, S. Yu, J. Xu and J. Liu, *ACS Nano*, 2015, **9**, 5461–5469.
42 Y. Huang, Z. Liu, C. Liu, E. Ju, Y. Zhang, J. Ren and X. Qu, *Angew. Chem., Int. Ed.*, 2016, **55**, 6646–6650.